nature neuroscience

Rapid production of new oligodendrocytes is required in the earliest stages of motor-skill learning

Lin Xiao[1,2,5], David Ohayon[1,4,5], Ian A McKenzie[1], Alexander Sinclair-Wilson[1], Jordan L Wright[1], Alexander D Fudge[1], Ben Emery[3], Huiliang Li[1,6] & William D Richardson[1,6]

We identified mRNA encoding the ecto-enzyme Enpp6 as a marker of newly forming oligodendrocytes, and used *Enpp6 in situ* hybridization to track oligodendrocyte differentiation in adult mice as they learned a motor skill (running on a wheel with unevenly spaced rungs). Within just 2.5 h of exposure to the complex wheel, production of *Enpp6*-expressing immature oligodendrocytes was accelerated in subcortical white matter; within 4 h, it was accelerated in motor cortex. Conditional deletion of myelin regulatory factor (*Myrf*) in oligodendrocyte precursors blocked formation of new *Enpp6*$^+$ oligodendrocytes and impaired learning within the same ~2–3 h time frame. This very early requirement for oligodendrocytes suggests a direct and active role in learning, closely linked to synaptic strengthening. Running performance of normal mice continued to improve over the following week accompanied by secondary waves of oligodendrocyte precursor proliferation and differentiation. We concluded that new oligodendrocytes contribute to both early and late stages of motor skill learning.

In the vertebrate central nervous system (CNS) many axons are ensheathed by myelin, tight spiral wraps of plasma membrane made by oligodendrocytes. Myelin greatly increases the speed of propagation of action potentials, permitting rapid information transfer over long distances and allowing the evolution of larger animals with bigger, more powerful brains. Approximately 5% of all neural cells in the rodent and human brain are oligodendrocyte precursors (OPs). These glial precursors generate the majority of myelinating oligodendrocytes during the early postnatal period (the first ~10 weeks in mice and 5–10 years in humans)[1,2], but continue to generate oligodendrocytes and myelin at a declining rate subsequently[2–9]. Differentiation of OPs into oligodendrocytes depends on the transcription factor Myrf[10,11]. Myrf is not expressed in cycling OPs but is first transcribed in differentiating oligodendrocytes, in which it is required for activation of many downstream genes including those encoding myelin structural proteins[10–12].

We previously investigated the function of adult-born oligodendrocytes in mice by inactivating *Myrf* conditionally in OPs, using tamoxifen-inducible *CreER*^{T2} under transcriptional control of platelet-derived growth factor receptor-alpha (*Pdgfra-CreER*^{T2}) to recombine and delete a *loxP*-flanked allele of *Myrf* (*P-Myrf*$^{-/-}$ mice)[13]. This dramatically reduced new oligodendrocyte production from their precursors without affecting preformed oligodendrocytes or myelin and prevented mice from mastering a new motor skill (running on a 'complex wheel' with irregular rung spacing). We concluded that development of new oligodendrocytes during adulthood is required for motor learning[13]. However, the precise role of new oligodendrocytes in the learning mechanism remains unclear. They might be needed in a purely permissive role; for example, to repair myelin that is lost or damaged in use, so that the underlying neural circuitry remains competent for learning. Alternatively, they might be involved more directly. For example, they might improve conduction by synthesizing myelin, by inducing sodium channels to cluster at 'pre-nodes' before myelination[14] or by transferring substrates for energy production (lactate and pyruvate) into axons[15,16]. Any or all of these mechanisms might improve the performance of new circuits while preserving them for future use.

A key component of learning at the subcellular level is synaptic modification[17–20]. This can occur very rapidly; there are dynamic changes to the number and size of dendritic spines (sites of synaptic contact) on pyramidal neurons in the mouse motor cortex within one-and-a-half hours of initiating fine-motor training[21]. This is much faster than previously reported responses of oligodendrocyte lineage cells to novel experience[13], or to other physiological or artificial stimuli[8,13,22,23], which have been reported to occur over days to weeks. This might suggest that oligodendrocytes act far downstream of synaptic change or in an entirely separate pathway. However, our knowledge of how oligodendrocyte lineage cells change in response to novel experience is still rudimentary, and more work is required before we can understand their role in neural plasticity.

To help elucidate the contribution of oligodendrocytes to motor learning, we examined the time course of learning and the accompanying cellular events at higher temporal resolution than has been done before. We analyzed complex wheel-running data for *P-Myrf*$^{-/-}$ mice

[1]Wolfson Institute for Biomedical Research, University College London, London, UK. [2]Institute of Neuroscience, Second Military Medical University, Shanghai, China. [3]Jungers Center for Neurosciences Research, Oregon Health and Science University, Portland, Oregon, USA. [4]Present address: Centre de Biologie du Développement, University Paul Sabatier, Toulouse, France. [5]These authors contributed equally to this work. [6]These authors jointly directed this work. Correspondence should be addressed to W.D.R. (w.richardson@ucl.ac.uk).

Received 23 December 2015; accepted 30 June 2016; published online 25 July 2016; doi:10.1038/nn.4351

and their *P-Myrf*$^{+/-}$ littermates and discovered that the performance of the two groups diverged very early, within 2–3 h of first introducing mice to the wheel. This result implies that oligodendrocyte differentiation is required at a very early stage of motor-skill learning, close to the point at which synaptic change occurs[21], suggesting that oligodendrocytes and myelin have a more active role in learning and memory than might have been imagined previously.

To look for direct evidence of early involvement of oligodendrocyte lineage cells, we analyzed OP proliferation and differentiation in the motor cortex and subcortical white matter of wild-type mice during the early stages of learning. Using a new molecular marker Enpp6 (a choline-specific ecto-nucleotide pyrophosphatase/phosphodiesterase)[24–26] that is preferentially expressed in early differentiating oligodendrocytes (ref. 27 and this work), we detected accelerated differentiation of OPs into newly forming oligodendrocytes after just 2.5 h self-training on the complex wheel. This early phase of oligodendrocyte production presumably involves direct differentiation of OPs that were paused in the G1 phase of the cell cycle before introduction of the wheel. The sudden surge of differentiation resulted in a transient dip in the local density (cells/mm^2) of OPs followed by increased S-phase entry among the remaining OPs and elevated oligodendrocyte production in the longer term (>10 d). Thus, it appears that a primary effect of novel experience is to stimulate rapid differentiation, within hours, of G1-arrested OPs into new oligodendrocytes that participate in and are required for optimal early stage learning. The subsequent wave of OP proliferation and differentiation, presumably a homeostatic reaction to the initial depletion of OPs[28], occurred together with continuing improvement in running performance, suggesting that the later-generated oligodendrocytes also contribute to learning and long-term motor memory.

RESULTS

Myrf is required in the first few hours of skill learning

We analyzed the ability of mice to run at speed on a complex wheel with irregularly spaced rungs, as described previously[13]. We assembled a large data set from tamoxifen-treated *Pdgfra-CreER*^{T2}*:Myrf*$^{loxP/loxP}$ mice (referred to as *P-Myrf*$^{-/-}$; $n = 32$; 17 males) and their *P-Myrf*$^{+/-}$ littermates ($n = 36$; 20 males), by combining data from several smaller cohorts of one or two litters each (postnatal day (P) 85 or P115 at the time of running). Mice ran mainly at night (during the dark part of the cycle; 6 p.m. to 6 a.m.) and were inactive in the day. As reported previously, both *P-Myrf*$^{+/-}$ and *P-Myrf*$^{-/-}$ mice improved their running speeds over a period of about 1 week, but the average or maximum speeds attained by *P-Myrf*$^{-/-}$ mice were always less than the control *P-Myrf*$^{+/-}$ group (ref. 13 and **Fig. 1a**; all mice received tamoxifen on four consecutive days, 3 weeks before running). At the end of the first night, performances of the two groups had already diverged, implying that Myrf-dependent processes were important during the first 12 h for optimal learning. Plotting average speed over successive 2-h (rather than 12-h) intervals showed that for both *P-Myrf*$^{-/-}$ and control groups most improvement during the first night occurred within the first 4 h, after which running performance leveled off (**Fig. 1b**). At the beginning of the second night, following 12 h of daytime inactivity and sleep, performance was immediately better than it had been at any time in the previous 24 h (**Fig. 1b**). This mirrored the sleep-dependent 'consolidation' that is observed in humans learning a motor task[29]. On subsequent nights, performance improved incrementally from one night to the next, beginning at a level close to the previous night's peak and improving further for a few hours before tailing off (**Fig. 1b** and **Supplementary Fig. 1**).

Plotting average running speed over 20-min intervals revealed that performance of *P-Myrf*$^{-/-}$ mice was already impaired relative to their *P-Myrf*$^{+/-}$ littermates within the first 2–3 h of the first night (**Fig. 1c**). This early requirement for Myrf presumably reflects differentiation of *Pdgfra*-expressing OPs into new oligodendrocytes; it cannot reflect modification or adaptation of preexisting oligodendrocytes or myelin because differentiated oligodendrocytes do not express *Pdgfra-CreER*^{T2} and therefore do not delete *Myrf*^{loxP}. OPs lacking *Myrf* do not differentiate properly but arrest and die before the expression of myelin structural genes[10,11,13].

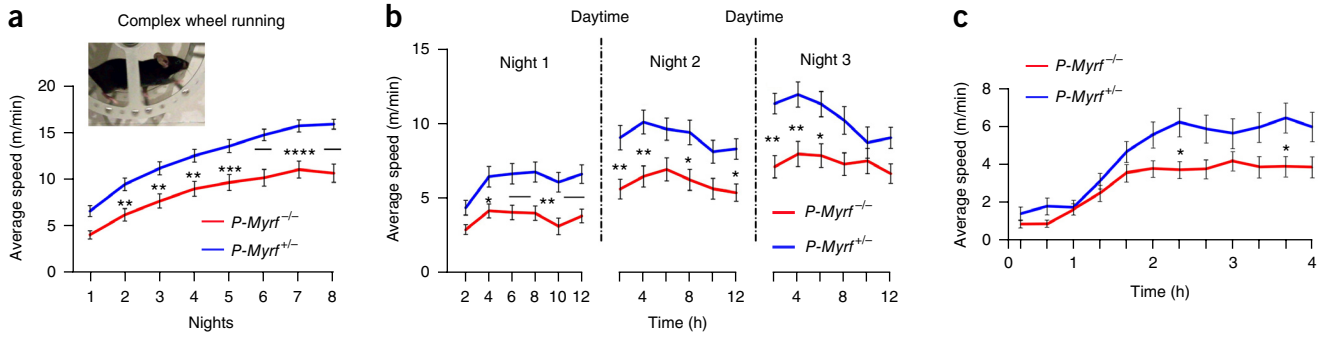

Figure 1 Time course of motor skill learning in mice and the requirement for *Myrf*. (**a**) Average speeds on complex wheel (pictured) during successive 24-h intervals of *P-Myrf*$^{-/-}$ mice ($n = 32$; 17 male) and their *P-Myrf*$^{+/-}$ littermates ($n = 36$, 20 male). (**b**) Average speeds during successive 2-h intervals during the first 3 d of the experiment. (**c**) Average speeds in 20-min intervals during the first 4 h of the first night. Data were analyzed by two-way ANOVA with Bonferroni's *post hoc* test. In **b**, each night was treated separately for multiple comparisons. Error bars indicate s.e.m. $^*P < 0.05$, $^{**}P < 0.01$, $^{***}P < 10^{-3}$, $^{****}P < 10^{-4}$. In **a**, night 1: $P = 0.09$, $t = 2.5$; night 2: $P = 0.01$, $t = 3.3$; night 3: $P = 0.004$, $t = 3.5$; night 4: $P = 0.004$, $t = 3.5$; night 5: $P = 0.0009$, $t = 3.9$; night 6: $P < 0.0001$, $t = 4.6$; night 7: $P < 10^{-4}$, $t = 4.7$; night 8: $P = 0.001$, $t = 3.8$. $F_{1,497} = 109.9$ and degrees of freedom (d.f.) = 497 throughout. In **b**, night 1: 2 h, $P = 0.43$, $t = 1.81$; 4 h, $P = 0.03$, $t = 2.8$; 6 h, $P = 0.009$, $t = 3.2$; 8 h, $P = 0.004$, $t = 3.4$; 10 h, $P = 0.002$, $t = 3.7$; 12 h, $P = 0.004$, $t = 3.5$. $F_{1,396} = 56.2$; night 2: 2 h, $P = 0.007$, $t = 3.3$; 4 h, $P = 0.003$, $t = 3.5$; 6 h, $P = 0.063$, $t = 2.6$; 8 h, $P = 0.015$, $t = 3.0$; 10 h, $P = 0.11$, $t = 2.4$; 12 h, $P = 0.03$, $t = 2.8$. $F_{1,396} = 51.1$; night 3: 2 h, $P = 0.002$, $t = 3.63$; 4 h, $P = 0.004$, $t = 3.43$; 6 h, $P = 0.02$, $t = 2.95$; 8 h, $P = 0.072$, $t = 2.53$; 10 h, $P > 0.99$, $t = 1.054$; 12 h, $P = 0.24$, $t = 2.06$. $F_{1,396} = 40.79$. d.f. = 396 throughout. In **c**, 20 min: $P > 0.99$, $t = 0.69$; 40 min: $P > 0.99$, $t = 0.10$; 60 min: $P > 0.99$, $t = 0.13$; 80 min: $P > 0.99$, $t = 0.81$; 100 min: $P > 0.99$, $t = 1.41$; 120 min: $P = 0.30$, $t = 2.44$; 140 min: $P = 0.022$, $t = 3.12$; 160 min: $P = 0.10$, $t = 1.83$; 180 min: $P = 0.83$, $t = 2.63$; 200 min: $P = 0.14$, $t = 2.63$; 220 min: $P = 0.017$, $t = 3.21$; 240 min: $P = 0.095$. $F_{1,792} = 42.32$ and d.f. = 792 throughout.

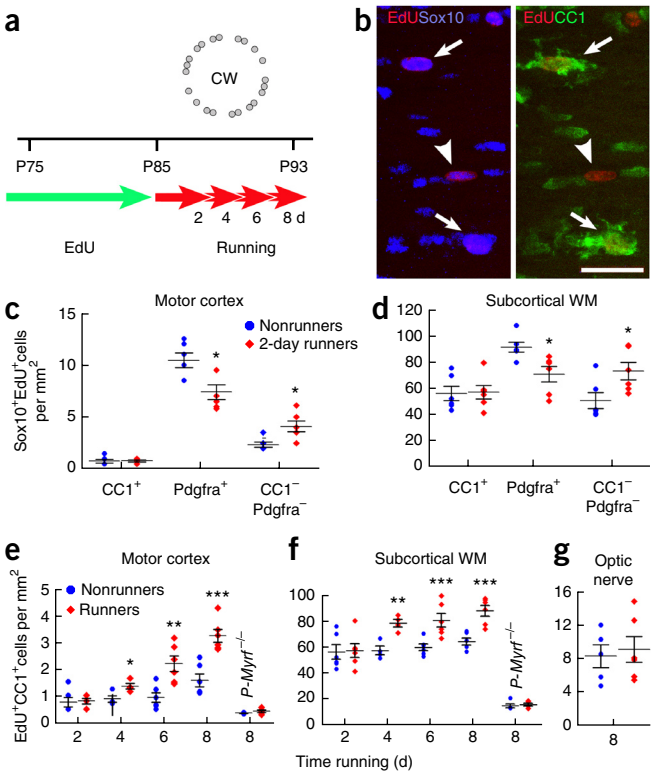

Figure 2 Oligodendrocyte dynamics during motor-skill learning. (**a**) Experimental design: all mice (approximately equal numbers of male and female) were given tamoxifen by gavage on 4 successive days (P60 to P63 inclusive), and then EdU was administered in the drinking water for 10 d (P75 to P84) before transferring the mice to cages equipped with a complex wheel (CW) for up to 8 d. (**b**) Double immunolabeling for Sox10 (left) and CC1 (right) combined with EdU detection (red) on a section of subcortical white matter of wild-type mice housed with a wheel for 8 d ('8-d runners'). ~97% of EdU$^+$ cells were also Sox10$^+$ oligodendrocyte lineage cells. There was a mixture of CC1-negative presumptive OPs (arrowheads) and CC1$^+$ newly formed oligodendrocytes (arrows). Images are representative of >3 similar experiments. Scale bar, 40 µm. (**c**,**d**) Numbers of newly generated (EdU$^+$) oligodendrocyte lineage cells at different developmental stages in 2-d runners vs. control littermates, housed without a wheel (nonrunners) in motor cortex (**c**) and underlying white matter (WM) (**d**). (**e**,**f**) Production of (EdU$^+$ CC1$^+$) new myelinating oligodendrocytes in motor cortex (**e**) and subcortical white matter (**f**) of runners vs. nonrunners. Number of new oligodendrocytes was strongly reduced in *P-Myrf*$^{-/-}$ mice, both runners and nonrunners, compared to wild-type mice (nonrunner 8 d, motor cortex: $P = 0.00091$, $t = -4.71$, d.f. = 9; sub-cortical white matter: $P < 10^{-5}$, $t = -15.43$, d.f. = 9; $n = 6$ for wild-type mice, $n = 5$ for *Myrf*$^{-/-}$ mice). (**g**) Production of new myelinating oligodendrocytes (EdU$^+$ CC1$^+$) in the optic nerve of runners vs. nonrunners ($P = 0.71$, $t = -0.39$, d.f. = 9, $n = 5$ runners, $n = 6$ nonrunners). Error bars, s.e.m.; $^*P < 0.05$, $^{**}P < 0.01$, $^{***}P < 0.001$; two-tailed unpaired *t*-test. In **c**, CC1$^+$, $P = 0.81$, $t = -0.25$; Pdgfra$^+$, $P = 0.012$, $t = 3.1$; Pdgfra$^-$ CC1$^-$, $P = 0.012$, $t = -3.1$, d.f. = 10, $n = 6$ mice. In **d**, CC1$^+$, $P = 0.90$, $t = -0.13$; Pdgfra$^+$, $P = 0.014$, $t = 2.94$; Pdgfra$^-$ CC1$^-$, $P = 0.012$, $t = 3.07$; d.f. = 10. $n = 6$ mice. In **e**, 2 d, $P = 0.90$, $t = -0.13$, d.f. = 10, $n = 6$ mice each group; 4 d, $P = 0.027$, $t = -2.90$, d.f. = 6, $n = 4$ mice each group; 6 d, $P = 0.0039$, $t = -3.73$, d.f. = 10, $n = 6$ mice each group; 8 d (WT), $P = 0.0006$, $t = -5.0$, d.f. = 10, $n = 6$ mice each group; 8 d (*Myrf*$^{-/-}$), $P = 0.18$, $t = -1.47$, d.f. = 8, $n = 6$ mice each group. In **f**, 2 d, $P = 0.61$, $t = -0.53$, d.f. = 10; $n = 6$ mice each group; 4 d, $P = 0.003$, $t = -4.8$, d.f. = 6, $n = 4$ mice each group; 6 d, $P = 0.0027$, $t = -3.54$, d.f. = 10, $n = 6$ mice each group; 8 d (wild type), $P = 0.0007$, $t = -4.82$, d.f. = 10, $n = 6$ mice each group; 8 d (*Myrf*$^{-/-}$), $P = 0.61$, $t = -0.53$, d.f. = 8, $n = 5$ mice each group.

Motor training accelerates OP differentiation

This rapid improvement in motor performance far preceded the running-induced OP proliferation that we had detected at 2–4 d in our previous study[13]. However, in that study we had administered the nucleotide analog 5-ethynyl-2′-deoxyuridine (EdU) from the time mice first encountered the wheel, so we could follow the fates only of those cells that entered S phase after that point. That could have limited our ability to detect the earliest cellular responses. Therefore, in new experiments we prelabeled wild-type mice with EdU for 10 d, from P75 to P85, before introducing the wheel (**Fig. 2a**). This was sufficient to label ~20% of OPs in the cortical gray matter and ~75% of OPs in the subcortical white matter (data not shown). We then followed the fates of those EdU-labeled cells in mice that had self-trained on the wheel for 48 h (P85–P87), by immunolabeling for Pdgfra to identify OPs and with monoclonal CC1 for oligodendrocytes. The majority of EdU$^+$ cells in both gray and white matter was also Sox10$^+$ (96.7% ± 0.6%; >1,000 cells counted in more than three sections from each of 3 mice, **Fig. 2b**), so EdU labeling can be used as a proxy oligodendrocyte lineage marker in these experiments. We observed a decrease in the

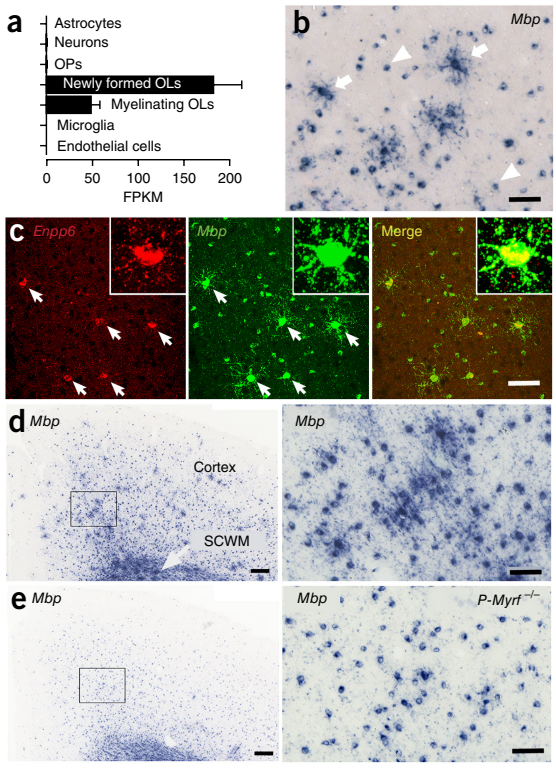

Figure 3 *Enpp6* marks newly forming oligodendrocytes. (**a**) *Enpp6* RNA-seq data adapted from ref. 27, http://web.stanford.edu/group/barres_lab/brain_rnaseq.html. OLs, oligodendrocytes; FPKM, fragments per kilobase of transcript per million mapped reads. Error bars, s.e.m. (**b**) ISH for *Mbp* transcripts on sections of P90 mouse motor cortex. Arrowheads indicate small cell bodies of mature oligodendrocytes; arrows indicate larger process-bearing 'spidery' cells, resembling 'premyelinating' oligodendrocytes described previously[30,31]. (**c**) Double ISH for *Mbp* and *Enpp6* showing that the spidery *Mbp*$^+$ cells (arrows) are also *Enpp6*$^+$. Insets, magnified images of right-most *Enpp6*^{high} cell. (**d**,**e**) ISH for *Enpp6* in forebrain sections of wild type (**d**) and *P-Myrf*$^{-/-}$ (**e**) mice. Boxed regions are magnified on the right. SCWM, subcortical white matter. Images are representative of >3 similar experiments. Scale bars, 50 µm (**b**, **c**, **d** right and **e** right) and 200 µm (**d** left and **e** left).

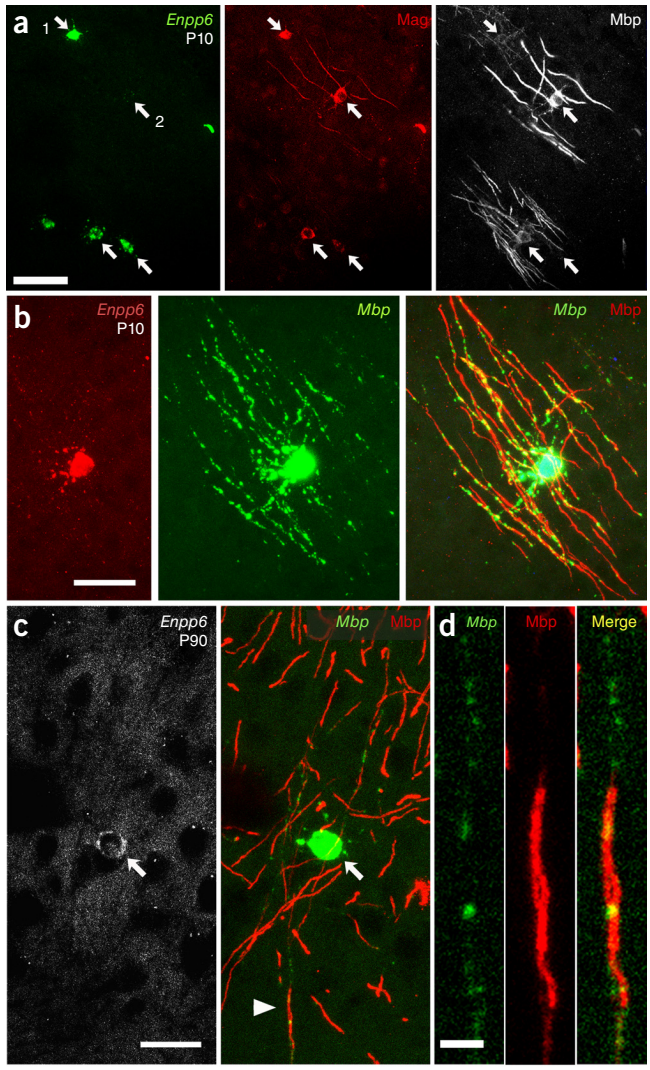

Figure 4 *Enpp6*^{high}*Mbp*$^{+}$ newly formed oligodendrocytes express myelin structural proteins and synthesize myelin. (**a**) ISH for *Enpp6* (left) followed by double immunolabeling for Mag (middle) and Mbp (right) in the P10 cortical gray matter. Arrows, cells expressing combinations of *Enpp6*, Mbp and Mag. 1, an *Enpp6*^{high} Mbp^{low} cell; 2, an *Enpp6*^{low} Mbp^{high} cell. (**b**) ISH for *Enpp6* (left) and *Mbp* (middle, green) followed by immunolabeling for Mbp (right, red) in the P10 cortex. *Mbp* mRNA is present in the cell body, radial processes and nascent myelin sheaths. (**c**,**d**) At P90, double ISH for *Enpp6* and *Mbp* (green) followed by immunolabeling for Mbp (red) identifies *Enpp6* cells that synthesize myelin sheaths. The cell shown is in motor cortex layer 2. Arrowhead in **c** marks the myelin sheath magnified in **d**. 'Spots' of *Mbp* mRNA (green) are visible in **d** where there is no Mbp^{+} myelin sheath (red); presumably these represent oligodendrocyte processes that are in contact with axons but have not yet translated myelin proteins (i.e., nascent myelin sheaths). Images are representative of >3 similar experiments. Scale bars, 50 μm (**a**–**c**) and 10 μm (**d**).

number density (cells per mm^2) of EdU^{+}Pdgfra^{+} OPs in mice housed with a wheel ('runners') relative to littermates housed without a wheel ('nonrunners') both in the motor cortex (7.3 ± 0.6 cells/mm^2 vs. 10.4 ± 0.7 in runners vs. nonrunners; P = 0.01, two-tailed unpaired t-test) and in subcortical white matter (71.2 ± 6.2 vs. 91.9 ± 4.0 cells/mm^2; P = 0.02; ≥3 sections analyzed from each of 6 mice) (**Fig. 2c**,**d**). This was accompanied by a reciprocal increase in the number density of EdU^{+}Sox10^{+} Pdgfra^{-}CC1^{-} cells, that is, newly differentiating oligodendrocytes that had lost Pdgfra but not yet acquired CC1 immunoreactivity (motor cortex: 4.1 ± 0.5 vs. 2.3 ± 0.2 cells/mm^2 in runners vs. nonrunners (P = 0.01); subcortical white matter: 73.5 ± 8.9 vs. 51.0 ± 5.5 cells/mm^2 (P = 0.03)) (**Fig. 2c**,**d**). These data demonstrate that novel experience with the complex wheel stimulated differentiation of OPs that had replicated their DNA in the 10 d before introduction to the wheel. At that time point (2 d with the wheel) there was no difference in the density of EdU^{+}CC1^{+} oligodendrocytes in runners vs. nonrunners (**Fig. 2c**–**e**), but a significant increase in density of those cells developed in runners between 2 d and 4 d, both in the motor cortex and subcortical white matter, and the increases persisted beyond 8 d (**Fig. 2e**,**f**). Numbers of EdU^{+}CC1^{+} newly formed oligodendrocytes decreased in *P-Myrf*$^{-/-}$ mice ($P < 0.10^{-4}$), as expected (**Fig. 2e**,**f**). There was no increase in oligodendrocyte production in the optic nerves of runners vs. nonrunners (**Fig. 2g**), demonstrating regional specificity of the response.

Enpp6, a new marker of newly forming oligodendrocytes

The cellular responses to wheel running after 2 d were still much delayed relative to the 2–3 h required to register an improvement in running performance (**Fig. 1c**). Nevertheless, the results described above drew our attention to the potential role of OP differentiation in early stages of learning. To facilitate study of early OP differentiation, we scanned existing expression databases for developmental-stage-specific markers and identified a gene, *Enpp6*, that is expressed highly in newly forming oligodendrocytes and at a much lower level in more mature myelinating oligodendrocytes, but not at all in OPs, neurons, astrocytes or vascular endothelial cells[27] (**Fig. 3a**). *In situ* hybridization (ISH) for *Enpp6* labeled cells in both the gray and white matter of the P60 mouse brain (**Supplementary Fig. 2**). We detected two populations of *Enpp6*-positive cells; the majority had small, weakly labeled cell bodies but a minor subpopulation had larger cell bodies that were more intensely labeled (**Fig. 3b** and **Supplementary Fig. 2**). This expression pattern is consistent with the interpretation that the numerous weakly labeled cells (*Enpp6*^{low}) are mature oligodendrocytes, whereas the less abundant strongly labeled cells (*Enpp6*^{high}) were newly differentiating, in keeping with the high-throughput RNA sequencing (RNA-seq) data[27].

By appropriately adjusting ISH conditions, we filtered out the weakly labeled cells and visualized only the strongly labeled, putative newly differentiating oligodendrocytes (**Supplementary Fig. 2b**). These *Enpp6*^{high} cells did not express *Pdgfra*, so they were not OPs, but they all had Sox10 and/or Olig2 immunoreactivity (**Supplementary Figs. 2c** and **3**, and **Supplementary Table 1**). Most but not all of them also labeled with CC1 (**Supplementary Fig. 3** and **Supplementary Table 1**), and they all expressed *Mbp* mRNA (**Fig. 3b**,**c** and **Supplementary Table 1**), which identified them as oligodendrocytes. At P90 the *Enpp6*^{high}*Mbp*$^{+}$ cells had a distinctive 'spidery' morphology with multiple radial processes (**Fig. 3b**,**c**). All *Enpp6*^{high} cells were *Mbp*$^{+}$ spidery cells and vice versa (**Fig. 3c** and **Supplementary Table 1**) and comprised < 5% of all *Mbp*$^{+}$ oligodendrocytes at P90. The *Enpp6*^{high}*Mbp*$^{+}$ spidery cells were practically absent from *P-Myrf*$^{-/-}$ brains (**Fig. 3d**,**e**), confirming that they were newly forming oligodendrocytes[13]. A morphological subclass of oligodendrocyte resembling the *Enpp6*^{high}*Mbp*$^{+}$ cells and described as 'premyelinating' has been visualized previously in rat and human brains, by immunolabeling for the myelin Proteolipid protein (Plp, DM20 isoform)[30,31].

We found that in P10 cerebral cortex, ~45% (66/146) of *Enpp6*^{high}*Mbp*$^{+}$ cells also expressed the myelin structural proteins

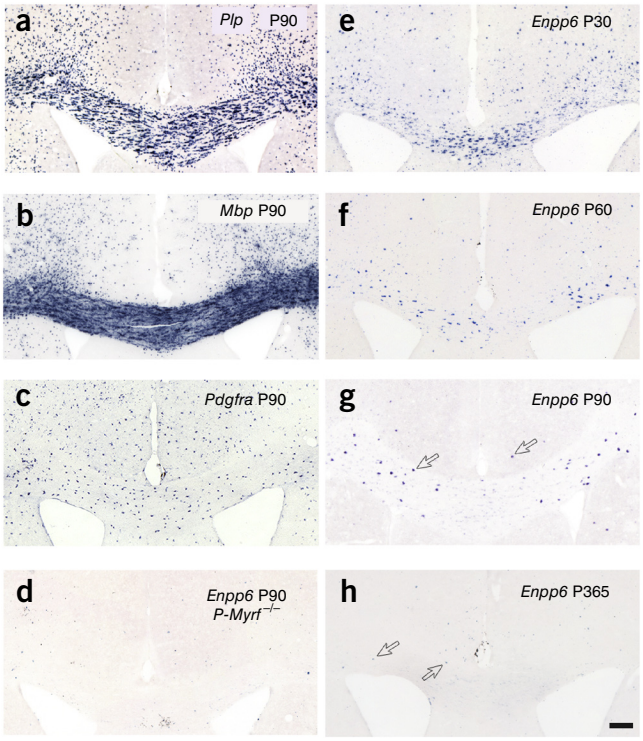

Figure 5 Visualization of *Enpp6*^{high} cells in the developing mouse forebrain by ISH. Forebrain sections of wild type (**a**–**c** and **e**–**h**) and *P-Myrf*$^{-/-}$ mice (**d**) were subjected to ISH for *Plp* (**a**), *Mbp* (**b**), *Pdgfra* (**c**) or *Enpp6* (**d**–**h**). Ages of the mice are indicated at the top right of each panel. Arrows in **g** and **h**, examples of *Enpp6*^{high} cells. Images are representative of >3 similar experiments. Scale bar, 100 µm.

myelin-associated glycoprotein (Mag) and Mbp in their cell bodies and processes, including myelin sheaths (**Fig. 4a**). Some of these (for example, cell 1 in **Fig. 4a**) expressed low amounts of Mbp protein, suggesting that they were newly myelinating. Those that expressed higher amounts of Mbp (for example, cell 2 in **Fig. 4a**) expressed low levels of *Enpp6*, consistent with *Enpp6* being downregulated as oligodendrocytes matured. Many *Enpp6*-expressing cells also expressed *Mbp* mRNA in their cell bodies as well as in their Mbp-positive myelin sheaths, both at P10 and P90 (**Fig. 4b**–**d**). At P90, in layer 2 of the motor cortex where myelin internodes were less dense and easier to associate with individual cell bodies, ~65% (37/55) of *Enpp6*^{high}*Mbp*$^{+}$ cells also expressed Mbp protein (**Fig. 4c**,**d**). We concluded that a substantial fraction of *Enpp6*^{high} cells in developing and adult brains synthesized nascent myelin sheaths.

The distribution pattern of *Enpp6*^{high} cells in the developing brain was distinct from that of either *Pdgfra*-expressing OPs or the general population of *Mbp*-expressing or *Plp*$^{+}$-expressing oligodendrocytes (**Fig. 5a**–**c**). They were almost completely absent from *P-Myrf*$^{-/-}$ brains (**Fig. 5d**), confirming that they are oligodendrocyte lineage cells. The number of *Enpp6*^{high} cells declined markedly with age, in keeping with the diminishing rate of oligodendrocyte differentiation[9] (**Fig. 5e**–**h**). *Enpp6*^{high} newly differentiating oligodendrocytes were still evident in the corpus callosum and cerebral cortex of young adult (P90) mice (**Fig. 5g**), and even at P365 we detected small numbers of these cells (**Fig. 5h**), consistent with a low rate of new oligodendrocyte production even at one year of age.

Enpp6 starts to be expressed after Pdgfra is extinguished and overlaps with the onset of CC1 expression, but is downregulated in more mature myelinating oligodendrocytes, which continue to express CC1 (**Supplementary Figs. 2** and **3**, and **Supplementary Table 1**). Therefore, *Enpp6*^{high} cells included some but not all Pdgfra^{-}CC1^{-} early differentiating oligodendrocytes (**Fig. 2**) as well as the earliest-forming CC1^{+} oligodendrocytes.

Accelerated production of Enpp6^{+} cells during training

We used ISH for *Enpp6* mRNA to detect newly differentiating oligodendrocytes in mice that were learning to run on the complex wheel (**Fig. 6a**–**i**). Within just 2.5 h, we detected an increase in the number of *Enpp6*^{high} cells in the subcortical white matter of runners vs. nonrunners (35.9 ± 2.0 cells/mm^2 vs. 28.4 ± 1.7 cells/mm^2; $P = 0.003$; ≥3 sections from each of 8 mice) (**Fig. 6k**). This increase in cell number occurred in the same time frame as the earliest improvements in running performance (**Fig. 1c**), consistent with the idea that new oligodendrocyte production is an integral part of early stage motor learning, occurring in parallel with, or closely following, changes at the level of synapses[21]. At 2.5 h we detected no change in *Enpp6*^{high} cells in the motor cortex of runners vs. nonrunners (**Fig. 6j**). However, at 4 h there was a ~25% increase in *Enpp6*^{high} cells in both motor cortex and subcortical white matter in runners vs. nonrunners (motor cortex: 12.9 ± 0.4 cells/mm^2 vs. 9.6 ± 0.6 cells/mm^2, $P < 0.001$; subcortical white matter: 40.5 ± 2.5 cells/mm^2 vs 29.4 ± 2.5 cells/mm^2, $P = 0.003$; ≥3 sections from each of 10 mice). After 12 h (one night) with the wheel, there was a ~50% increase in *Enpp6*^{high} cells in runners vs. nonrunners (motor cortex, 15.7 ± 0.6 cells/mm^2 vs. 9.6 ± 0.4 cells/mm^2, $P < 0.001$; subcortical white matter: 48.7 ± 2.4 cells/mm^2 vs. 29.4 ± 1.7 cells/mm^2, $P < 0.001$) and after another 12 h (i.e., one night plus the following daytime inactivity period) an even larger (about twofold) increase (motor cortex: 23.3 ± 1.2 cells/mm^2 vs. 10.7 ± 1.1 cells/mm^2, $P < 0.001$; subcortical white matter: 54.2 ± 7.9 cells/mm^2 vs. 27.9 ± 2.2 cells/ mm^2, $P < 0.001$) (**Fig. 6j**,**k**). The latter data raise the possibility that the improvement in running performance that develops during sleep or inactivity (**Fig. 1c**) might be related to ongoing oligodendrocyte generation; it has been reported that OP proliferation and differentiation is circadian, with S-phase entry occurring preferentially during the day and M phase and oligodendrocyte differentiation at night[32,33]. Production of *Enpp6*^{high} cells was dramatically reduced in *P-Myrf*$^{-/-}$ mice relative to wild-type mice both in nonrunners and 12-h runners (**Fig. 6c**,**f**,**i**–**k**), as expected. We still observed increased numbers of newly formed *Enpp6*^{high} oligodendrocytes in 8-d runners, though in reduced numbers compared to earlier time points (**Fig. 6j**,**k**).

Motor learning, not exercise, stimulates oligodendrogenesis

Increased oligodendrocyte differentiation might conceivably have been part of a systemic response to exercise, rather than to motor learning per se. To disentangle these effects, we compared two cohorts of wild-type mice, one of which self-trained on the complex wheel for 8 d, rested for 2 weeks, and then was reintroduced to the complex wheel for 24 h. The other cohort we introduced to the complex wheel once only, for 24 h (**Fig. 7a**). The average running speed and distance traveled over 24 h of the latter group (here referred to as 'first-timers') was much less than that for the second-timers that had already mastered the wheel 2 weeks previously (**Fig. 7b**,**c**). Despite this, the *Enpp6*^{high} number density was increased in motor cortex and underlying white matter only in the first-timers (**Fig. 7d**,**e**). This experiment dissociates running speed (physical exercise) from novel running experience (learning) and demonstrated that the rate of production of new oligodendrocytes increased only during the primary learning event.

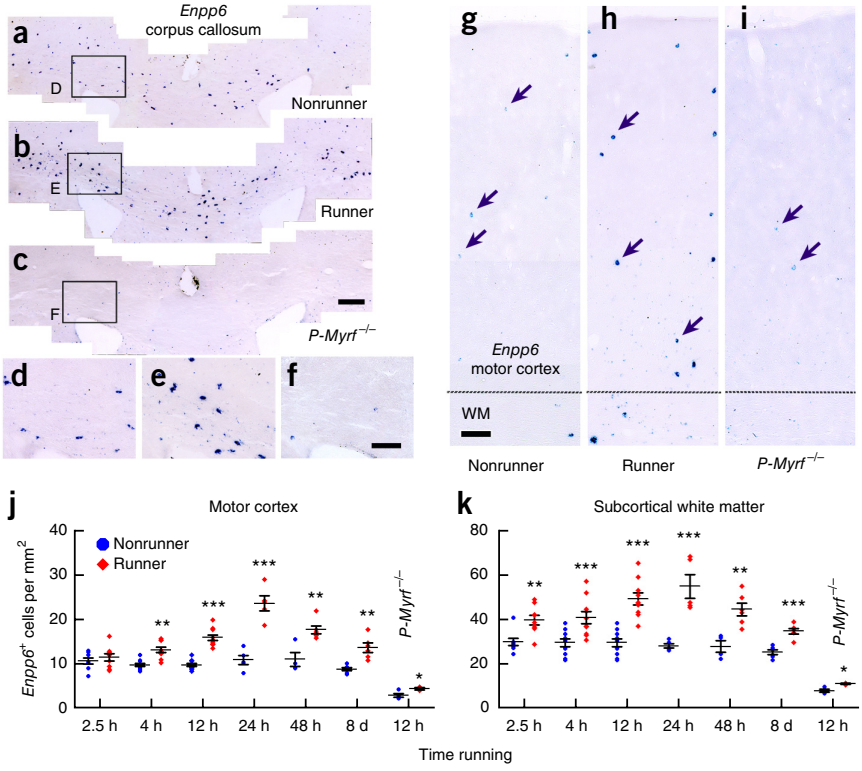

Figure 6 Rapid increase in *Enpp6*^{high} newly forming oligodendrocytes in response to motor-skill learning. (**a**–**i**) ISH for *Enpp6* in sections of nonrunner, runner (24 h with the complex wheel) and *P-Myrf*$^{-/-}$ (nonrunner) subcortical white matter (**a**–**f**) or motor cortex (**g**–**i**). Magnification of boxed areas in **a**–**c** is shown in **d**–**f**, respectively. Scale bars, 200 μm (**a**–**c**) and 100 μm (**d**–**i**). Arrows, examples of *Enpp6*^{high} cells. Dashed line, boundary between gray and white matter (WM). Images are representative of >3 similar experiments. (**j**,**k**) Quantification of *Enpp6*^{high} cells in wild-type or *P-Myrf*$^{-/-}$ mice housed with or without a complex wheel for indicated durations. Numbers of *Enpp6*^{high} cells were greatly decreased in *P-Myrf*$^{-/-}$ compared to wild-type mice, (nonrunner 12 h, (**j**) motor cortex: $P < 10^{-5}$, $t = -13.37$, d.f. = 12; (**k**) subcortical white matter: $P < 10^{-5}$, $t = -11.28$, d.f. = 12; $n = 10$ for wild-type mice, $n = 4$ for *Myrf*$^{-/-}$ mice). Error bars, s.e.m. $^{*}P < 0.05$, $^{**}P < 0.01$, $^{***}P < 0.001$, comparing runners with nonrunners using two-tailed unpaired *t*-test. WM, white matter. In **j**, 2.5 h, $P = 0.43$, $t = -0.81$, d.f. = 15, $n = 8$ mice for nonrunners, $n = 9$ mice for runners; 4 h, $P = 9 \times 10^{-5}$, $t = -5.024$, d.f. = 18, $n = 10$ mice each group; 12 h (wild type), $P < 10^{-5}$, $t = -8.50$, d.f. = 18, $n = 10$ mice each group; 24 h, $P = 0.00019$, $t = -6.46$, d.f. = 8, $n = 5$ mice each group; 48 h, $P = 0.0038$, $t = 4.03$, d.f. = 9, $n = 4$ mice for nonrunners, $n = 6$ for runners; 8 d, $P = 0.0013$, $t = -4.42$, d.f. = 10, $n = 6$ mice each group; 12 h (*Myrf*$^{-/-}$), $P = 0.049$, $t = -2.59$, d.f. = 5, $n = 4$ mice for nonrunners, $n = 3$ mice for runners. In **k**, 2.5 h, $P = 0.0026$, $t = -3.60$, d.f. = 15, $n = 8$ mice for nonrunners, $n = 9$ mice for runners; 4 h, $P = 0.0026$, $t = -3.50$, d.f. = 18, $n = 10$ mice each group; 12 h (wild type), $P < 10^{-5}$, $t = -6.20$, d.f. = 18, $n = 10$ mice each group; 24 h, $P = 0.001$, $t = -5.06$, d.f. = 8, $n = 5$ mice each group; 48 h, $P = 0.0038$, $t = 4.03$, d.f. = 8, $n = 4$ mice for nonrunners, $n = 6$ for runners; 8 d, $P = 2 \times 10^{-5}$, $t = -5.71$, d.f. = 10, $n = 6$ mice each group; 12 h (*Myrf*$^{-/-}$), $P = 0.013$, $t = -3.77$, d.f. = 5, $n = 4$ mice for nonrunners, $n = 3$ mice for runners.

Moreover, increased production of *Enpp6*^{high} newly differentiating oligodendrocytes was induced in motor cortex but not visual cortex of the first-timers in this experiment (**Fig. 7f**), demonstrating regional specificity of the early learning response.

DISCUSSION

We presented evidence that oligodendrocyte development was required for motor learning in adult mice, within the first few hours of their being introduced to the complex running wheel. The performance of *P-Myrf*$^{-/-}$ and *P-Myrf*$^{+/-}$ groups both started out at baseline, but mice in the two groups improved at different rates over the first 2–3 h, before equilibrating at different levels. This observation reinforced our conclusion that the two groups learned at different rates, rather than possessing inherently different physical abilities, as the physical effort required for the initial low-speed wheel-turning was unlikely to be limiting. At the cellular level, the primary response was accelerated production of *Enpp6* and *Mbp*-expressing early differentiating (spidery) oligodendrocytes, which we detected within the first 2.5 h (**Supplementary Fig. 4**). This might underestimate the rapidity of the response, as *Enpp6* does not mark the very earliest differentiating

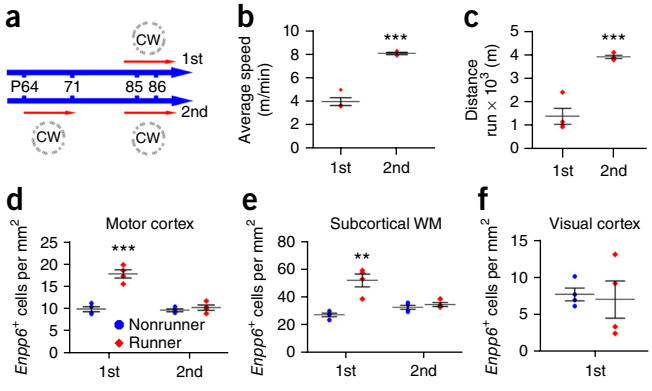

Figure 7 Increased production of *Enpp6*$^{+}$ newly formed oligodendrocytes was a response to motor learning, not physical exercise. (**a**) Experimental design, in which one group of mice (2nd) self-trained on the complex wheel (CW) for 1 week, rested for 2 weeks, and then was reintroduced to the wheel along with a separate group that was introduced for the first time (1st). After 24 h (P85–P86) both groups of mice (and parallel groups of nonrunners) were analyzed by ISH for *Enpp6*. (**b**) Average speeds (m/min) of first-timers (1st) and second-timers (2nd) during the 48 h P85–P86. (**c**) Distances run by 1st and 2nd during P85–P86. (**d**,**e**) Number densities (cells per mm^2) of *Enpp6*^{high} newly formed oligodendrocytes in 1st and 2nd after running on the complex wheel for 48 h (P85–P86), versus age-matched nonrunner controls, in motor cortex (**d**) and subcortical white matter (**e**). (**f**) New *Enpp6*^{high} oligodendrocyte production in the visual cortex in 1st versus age-matched nonrunner controls. $n = 4$ mice in each group. Error bars, s.e.m. $^{*}P < 0.05$, $^{**}P < 0.01$, $^{***}P < 0.001$; two-tailed unpaired *t*-test. In **b**, $P = 10^{-5}$, $t = -11.72$, d.f. = 6. In **c**, $P = 0.00035$, $t = -7.23$, d.f. = 6. In **d**, 1st, $P = 0.00033$, $t = -7.29$, d.f. = 6; 2nd, $P = 0.38$, $t = -0.95$, d.f. = 6. In **e**, 1st, $P = 0.0021$, $t = -5.16$, d.f. = 6; 2nd, $P = 0.34$, $t = -1.03$, d.f. = 6. In **f**, $P = 0.80$, $t = 0.27$, d.f. = 6.

cells; there was still a gap between downregulation of *Pdgfra* and appearance of *Enpp6* (**Supplementary Fig. 4**). The rapid increase in *Enpp6*-expressing newly forming oligodendrocytes is likely to result from stimulated differentiation of G1-phase-paused OPs, because at 2 d of training we observed a reduction in the absolute number of OPs (**Fig. 2c**,**d**); however, it is possible that increased survival of *Enpp6*-expressing cells also played a part. Production of *Enpp6*^{high} newly forming oligodendrocytes peaked around 24 h and declined thereafter, although increased production was still evident after 8 d. We observed that peak of new oligodendrocyte production only during the first encounter with the wheel, not during a subsequent encounter, and only in motor cortex and not visual cortex, suggesting that it is a specific response to motor learning, not exercise *per se*.

The early surge of OP differentiation was reflected in a reduction at 2 d of running in the number of OPs (prelabeled with EdU) and a corresponding increase in the number of Pdgfra^{-}CC1^{-} newly forming oligodendrocytes. This was followed at 2–4 d by accelerated S-phase entry of some of the remaining OPs[13]. This sequence suggests that the S-phase entry observed at 2–4 d was a homeostatic response to the earlier depletion of OPs through differentiation. For example, local depletion of OPs could result in loss of contact inhibition[28] or a local excess (through reduced consumption) of a mitogenic growth factor (for example, Pdgf)[34], either or both of which might stimulate proliferation of the remaining OPs in the locality. This spike of OP generation propelled a secondary wave of oligodendrocyte production over the following days to weeks (**Figs. 2d** and **4g**,**h** and ref. 13). The dynamics of the system are complex, and it seems likely that oligodendrocytes contribute to motor-skill acquisition in different ways at different stages of the process.

Various learning regimens in humans and rodents are associated with changes to the microstructure of gray and white matter, detected by magnetic resonance diffusion tensor imaging. For example, people or rats learning a complex visuomotor skill (for example, juggling or using an abacus for humans, and grasping food pellets for rats) develop altered microstructure in the motor cortex and/or subcortical white matter after training for days to weeks[35–38]. Changes to gray and white matter microstructure can be detected even within 2 h in people learning to play an action video game[39]. Experience-dependent structural changes to gray and/or white matter could in principle result from synaptogenesis and elaboration of the dendritic arbor[17–21], alterations to astrocyte morphology and their interactions with neurons[40], changes to the microvasculature[41] or altered (adaptive) myelination[22,23,42,43]. The results of our own present and previous studies[13] support the latter possibility.

Our ability to detect early oligodendrocyte dynamics relied partly on Enpp6, which we characterized as a new marker of early differentiating oligodendrocytes. Enpp6 is likely to become a useful tool for studying oligodendrocyte differentiation *in vivo*; for example, during remyelination of demyelinated lesions. Enpp6 is considered to be a choline-specific glycerophosphodiester phosphodiesterase, as it can hydrolyze glycerophosphocholine and sphingosylphosphocholine efficiently *in vitro*[24–26]. Therefore, it seems likely that Enpp6 has a role in lipid metabolism during formation of the myelin sheath and might be required to initiate myelination rapidly in response to differentiation-inducing signals, including those that operate during motor learning. It will be interesting in future to examine the functional role of Enpp6 and related family members during myelination.

How might newly forming oligodendrocytes contribute to learning? The rapidity of their formation suggests that they work in close partnership with neurons, hand-in-hand with (or close on the heels of) synaptic change, not simply by preserving or 'ossifying' new circuits after they have become established. For example, when mice first encountered the complex wheel they tried to develop strategies for coping with unequal rung spacing; this presumably involves exploratory firing of distinct neurons or groups of neurons along the motor pathways. There might be several or many parallel circuits that can generate behavioral outputs within a useful range, some more effective than others. The superior circuit(s) might be activated more frequently than others as the action is rehearsed, and thus become selected and strengthened according to Hebbian principles, both at the level of the synapse and by rapid and selective myelination of the interconnecting axons. It is known that OPs receive synaptic input from axons[44], and that oligodendrocyte development and myelination can be regulated by axonal activity *in vivo*[22,23,42–46]. Newly differentiating oligodendrocytes might enhance circuit function by initiating myelination and/or clustering of sodium channels and other nodal components before myelination[14], by supporting axonal metabolism[15,16], or a combination of those effects. This in turn could enhance connectivity at the synaptic level and so on, back and forth. As myelin thickness and compaction increases, the performance of the network and its behavioral outputs would be expected to improve further. Therefore, oligodendrocytes are likely to contribute to learning over an extended period from hours to weeks. Ultimately, myelin protects axons metabolically and physically over the long term, preserving lifelong memories.

METHODS

Methods and any associated references are available in the online version of the paper.

Note: Any Supplementary Information and Source Data files are available in the online version of the paper.

ACKNOWLEDGMENTS

We thank our colleagues at University College London, especially S. Jolly, U. Grazini and L. Magno, for advice and reagents, and M. Grist and U. Dennehy for technical help. We thank M. Wegner (University of Erlangen, Germany) for the Sox10 antibody. This work was supported by the European Research Council (grant agreement 293544 to W.D.R.), the Wellcome Trust (100269/Z/12/Z to W.D.R.) and the Biotechnology and Biological Sciences Research Council (BB/L003236/1 to H.L.). L.X. was supported by the National Natural Science Foundation of China (grant 31471013). *Pdgfra-CreER*^{T2} mice can be obtained through http://www.e-lucid.com/ with a material transfer agreement. *Myrf*^{loxP} mice are available from Jackson Labs, strain 010607.

AUTHOR CONTRIBUTIONS

W.D.R. formed the hypotheses and obtained funding. I.A.M. adopted and developed the complex wheel test. B.E. provided *Myrf*^{loxP} mice, advice and suggestions. W.D.R., I.A.M. and D.O. designed the experiments in **Figure 1** and **Supplementary Figure 1**; D.O. and I.A.M. performed those experiments and DO analyzed the data. W.D.R., H.L. and L.X. designed all the other experiments and L.X. performed them, with assistance from A.S.-W., J.L.W. and A.D.F. H.L. identified *Enpp6* and A.F. performed preliminary characterization. H.L. and W.D.R. supervised the work. W.D.R. wrote the paper with input from H.L., L.X. and B.E.

COMPETING FINANCIAL INTERESTS

The authors declare no competing financial interests.

1. Sturrock, R.R. Myelination of the mouse corpus callosum. *Neuropathol. Appl. Neurobiol.* **6**, 415–420 (1980).
2. Yeung, M.S. *et al.* Dynamics of oligodendrocyte generation and myelination in the human brain. *Cell* **159**, 766–774 (2014).
3. Dimou, L., Simon, C., Kirchhoff, F., Takebayashi, H. & Götz, M. Progeny of Olig2-expressing progenitors in the gray and white matter of the adult mouse cerebral cortex. *J. Neurosci.* **28**, 10434–10442 (2008).
4. Rivers, L.E. *et al.* PDGFRA/NG2 glia generate myelinating oligodendrocytes and piriform projection neurons in adult mice. *Nat. Neurosci.* **11**, 1392–1401 (2008).

5. Lasiene, J., Matsui, A., Sawa, Y., Wong, F. & Horner, P.J. Age-related myelin dynamics revealed by increased oligodendrogenesis and short internodes. *Aging Cell* **8**, 201–213 (2009).
6. Kang, S.H., Fukaya, M., Yang, J.K., Rothstein, J.D. & Bergles, D.E. NG2^{+} CNS glial progenitors remain committed to the oligodendrocyte lineage in postnatal life and following neurodegeneration. *Neuron* **68**, 668–681 (2010).
7. Zhu, X. *et al.* Age-dependent fate and lineage restriction of single NG2 cells. *Development* **138**, 745–753 (2011).
8. Simon, C., Götz, M. & Dimou, L. Progenitors in the adult cerebral cortex: cell cycle properties and regulation by physiological stimuli and injury. *Glia* **59**, 869–881 (2011).
9. Young, K.M. *et al.* Oligodendrocyte dynamics in the healthy adult CNS: evidence for myelin remodeling. *Neuron* **77**, 873–885 (2013).
10. Emery, B. *et al.* Myelin gene regulatory factor is a critical transcriptional regulator required for CNS myelination. *Cell* **138**, 172–185 (2009).
11. Koenning, M. *et al.* Myelin gene regulatory factor is required for maintenance of myelin and mature oligodendrocyte identity in the adult CNS. *J. Neurosci.* **32**, 12528–12542 (2012).
12. Hornig, J. *et al.* The transcription factors Sox10 and Myrf define an essential regulatory network module in differentiating oligodendrocytes. *PLoS Genet.* **9**, e1003907 (2013).
13. McKenzie, I.A. *et al.* Motor skill learning requires active central myelination. *Science* **346**, 318–322 (2014).
14. Freeman, S.A. *et al.* Acceleration of conduction velocity linked to clustering of nodal components precedes myelination. *Proc. Natl. Acad. Sci. USA* **112**, E321–E328 (2015).
15. Fünfschilling, U. *et al.* Glycolytic oligodendrocytes maintain myelin and long-term axonal integrity. *Nature* **485**, 517–521 (2012).
16. Lee, Y. *et al.* Oligodendroglia metabolically support axons and contribute to neurodegeneration. *Nature* **487**, 443–448 (2012).
17. Volkmar, F.R. & Greenough, W.T. Rearing complexity affects branching of dendrites in the visual cortex of the rat. *Science* **176**, 1445–1447 (1972).
18. Bliss, T.V. & Collingridge, G.L. A synaptic model of memory: long-term potentiation in the hippocampus. *Nature* **361**, 31–39 (1993).
19. Milner, B., Squire, L.R. & Kandel, E.R. Cognitive neuroscience and the study of memory. *Neuron* **20**, 445–468 (1998).
20. Lee, K.J., Rhyu, I.J. & Pak, D.T. Synapses need coordination to learn motor skills. *Rev. Neurosci.* **25**, 223–230 (2014).
21. Xu, T. *et al.* Rapid formation and selective stabilization of synapses for enduring motor memories. *Nature* **462**, 915–919 (2009).
22. Li, Q., Brus-Ramer, M., Martin, J.H. & McDonald, J.W. Electrical stimulation of the medullary pyramid promotes proliferation and differentiation of oligodendrocyte progenitor cells in the corticospinal tract of the adult rat. *Neurosci. Lett.* **479**, 128–133 (2010).
23. Gibson, E.M. *et al.* Neuronal activity promotes oligodendrogenesis and adaptive myelination in the mammalian brain. *Science* **344**, 1252304 (2014).
24. Greiner-Tollersrud, L., Berg, T., Stensland, H.M., Evjen, G. & Greiner-Tollersrud, O.K. Bovine brain myelin glycerophosphocholine choline phosphodiesterase is an alkaline lysosphingomyelinase of the eNPP-family, regulated by lysosomal sorting. *Neurochem. Res.* **38**, 300–310 (2013).
25. Sakagami, H. *et al.* Biochemical and molecular characterization of a novel choline-specific glycerophosphodiester phosphodiesterase belonging to the nucleotide pyrophosphatase/phosphodiesterase family. *J. Biol. Chem.* **280**, 23084–23093 (2005).
26. Morita, J. *et al.* Structure and biological function of ENPP6, a choline-specific glycerophosphodiester-phosphodiesterase. *Sci. Rep.* **6**, 20995 (2016).
27. Zhang, Y. *et al.* An RNA-sequencing transcriptome and splicing database of glia, neurons, and vascular cells of the cerebral cortex. *J. Neurosci.* **34**, 11929–11947 (2014).
28. Hughes, E.G., Kang, S.H., Fukaya, M. & Bergles, D.E. Oligodendrocyte progenitors balance growth with self-repulsion to achieve homeostasis in the adult brain. *Nat. Neurosci.* **16**, 668–676 (2013).
29. Walker, M.P., Brakefield, T., Morgan, A., Hobson, J.A. & Stickgold, R. Practice with sleep makes perfect: sleep-dependent motor skill learning. *Neuron* **35**, 205–211 (2002).
30. Trapp, B.D., Nishiyama, A., Cheng, D. & Macklin, W. Differentiation and death of premyelinating oligodendrocytes in developing rodent brain. *J. Cell Biol.* **137**, 459–468 (1997).
31. Chang, A., Tourtellotte, W.W., Rudick, R. & Trapp, B.D. Premyelinating oligodendrocytes in chronic lesions of multiple sclerosis. *N. Engl. J. Med.* **346**, 165–173 (2002).
32. Matsumoto, Y. *et al.* Differential proliferation rhythm of neural progenitor and oligodendrocyte precursor cells in the young adult hippocampus. *PLoS One* **6**, e27628 (2011).
33. Bellesi, M. Sleep and oligodendrocyte functions. *Curr Sleep Med Rep.* **1**, 20–26 (2015).
34. van Heyningen, P., Calver, A.R. & Richardson, W.D. Control of progenitor cell number by mitogen supply and demand. *Curr. Biol.* **11**, 232–241 (2001).
35. Draganski, B. *et al.* Neuroplasticity: changes in grey matter induced by training. *Nature* **427**, 311–312 (2004).
36. Scholz, J., Klein, M.C., Behrens, T.E. & Johansen-Berg, H. Training induces changes in white-matter architecture. *Nat. Neurosci.* **12**, 1370–1371 (2009).
37. Hu, Y. *et al.* Enhanced white matter tracts integrity in children with abacus training. *Hum. Brain Mapp.* **32**, 10–21 (2011).
38. Sampaio-Baptista, C. *et al.* Motor skill learning induces changes in white matter microstructure and myelination. *J. Neurosci.* **33**, 19499–19503 (2013).
39. Sagi, Y. *et al.* Learning in the fast lane: new insights into neuroplasticity. *Neuron* **73**, 1195–1203 (2012).
40. Ho, V.M., Lee, J.A. & Martin, K.C. The cell biology of synaptic plasticity. *Science* **334**, 623–628 (2011).
41. Kole, K. Experience-dependent plasticity of neurovascularization. *J. Neurophysiol.* **114**, 2077–2079 (2015).
42. Makinodan, M., Rosen, K.M., Ito, S. & Corfas, G. A critical period for experience-dependent oligodendrocyte maturation and myelination. *Science* **337**, 1357–1360 (2012).
43. Mangin, J.M., Li, P., Scafidi, J. & Gallo, V. Experience-dependent regulation of NG2 progenitors in the developing barrel cortex. *Nat. Neurosci.* **15**, 1192–1194 (2012).
44. Bergles, D.E. & Richardson, W.D. Oligodendrocyte development and plasticity. in *Glia* (eds. Barres, B.A., Freeman, M.R. & Stevens, B.) 139–165 (Cold Spring Harbor, 2015).
45. Hines, J.H., Ravanelli, A.M., Schwindt, R., Scott, E.K. & Appel, B. Neuronal activity biases axon selection for myelination *in vivo*. *Nat. Neurosci.* **18**, 683–689 (2015).
46. Mensch, S. *et al.* Synaptic vesicle release regulates myelin sheath number of individual oligodendrocytes *in vivo*. *Nat. Neurosci.* **18**, 628–630 (2015).

ONLINE METHODS

Mice. *Myrf*$^{loxP/loxP}$ mice were imported to University College London (UCL) originally (in 2010) on a mixed 129/CBA/C57B6 background. After crossing into a homozygous *Pdgfra-CreER*^{T2} background (predominantly C57B6; three generations) they have been maintained by sibling crosses for more than six generations and now generate exclusively agouti offspring. They are therefore mixed C57B6/CBA/129 with the major contribution being C57B6 (though agouti coat color is CBA-derived). Generation and genotyping of *Pdgfra-CreER*^{T2}*:Myrf*$^{loxP/loxP}$ and *Pdgfra-CreER*^{T2}*: Myrf*$^{+/loxP}$ littermates has been described[13]. Tamoxifen (Sigma) was dissolved at 40 mg/ml in corn oil by sonicating at 21 °C for 1 h. It was administered to mice (both *Myrf* $^{loxP/loxP}$ and *Myrf*$^{+/loxP}$) by oral gavage on four consecutive days ending on P64 (four cohorts) or P94 (one cohort) to induce recombination and deletion of *Myrf* in Pdgfra$^+$ OPs (each dose was 300 mg/kg body weight). This generated *P-Myrf*$^{-/-}$ and *P-Myrf*$^{+/-}$ mice for behavioral experiments. Mice were rested 3 weeks between the last tamoxifen dose and being introduced to the complex wheel at P85 or P115 (ref. 13). Wild-type mice were C57B6 (Charles River). All animal experiments were preapproved by the UCL Ethical Committee and authorized by the Home Office of the UK Government.

The complex wheel. We purchased wheel cages (Lafayette Neuroscience) that allow digital recording of wheel rotation speed over time (using an infrared beam) for more than 20 cages simultaneously. Complex wheels were made by removing 16 rungs from 38-rung, 12.7 cm diameter regular wheels, creating a 19-rung repeating pattern[13]. Mice were maintained on a 12-h artificial light-dark cycle, caged singly with the wheel and a small amount of nesting material (tissue paper). During running experiments, food and water was replenished every 48 h (during the light/inactivity cycle) but otherwise the mice were not disturbed. For comparison of *P-Myrf*$^{-/-}$ and *P-Myrf*$^{+/-}$ mice, wheel speed was measured once per hour during the light/inactive period and at 1-min intervals during the dark/active period, and data were exported automatically to a spreadsheet. Average wheel speeds were calculated for successive time intervals (12 h, 2 h or 20 min) and compared by two-way analysis of variance (ANOVA) with Bonferroni's *post hoc* tests using GraphPad Prism 6.0 software.

Histology and cell counts. Mice were perfusion-fixed with 4% (w/v) paraformaldehyde (PFA; Sigma) in diethylpyrocarbonate (DEPC)-treated phosphate-buffered saline (PBS). Brain tissue was dissected and post-fixed in 4% PFA overnight at 4 °C. Tissue was cryoprotected in 20% (w/v) sucrose (Sigma) in PBS before freezing in OCT on the surface of dry ice. Coronal cryosections (20 µm) of the brain were collected and processed as floating sections. Primary and secondary antibodies were diluted in blocking solution (0.1% (v/v) Triton X-100, 10% (v/v) FCS in PBS) and applied to sections overnight at 4 °C. Primary antibodies were anti-PDGFRa (rabbit, New England BioLabs catalog number 3164S, 1:500 dilution), anti-Olig2 (rabbit, Abcam AB9610, 1:400), anti-Sox10 (guinea pig, 1:2,000; a gift from M. Wegner), monoclonal CC1 (mouse, Calbiochem OP80,1:200), anti-Mag (mouse, Abcam ab89780, 1:200) and anti-Mbp (rat, AbD Serotec MCA409S, 1:200).

Low-magnification (20× objective) confocal images were collected using a Leica SPE laser-scanning confocal microscope as *Z* stacks with 1-µm spacing, using standard excitation and emission filters for DAPI, FITC (Alexa Fluor 488), TRITC (Alexa Fluor 568) and Far Red (Alexa Fluor 647). Cells were counted in non-overlapping fields of coronal sections of the corpus callosum or motor cortex, between the dorsolateral corners of the lateral ventricles (six fields per section, three sections from each of three or more mice of a given experimental group).

EdU labeling *in vivo*. Mice were given 5-ethynyl-2′-deoxyuridine (EdU) in their drinking water (0.2 mg/ml)[9] for 10 d from P75-P85. The animals were caged with a complex wheel for different durations, and then were perfusion-fixed and analyzed by immunolabeling floating cryosections (20 µm) with monoclonal CC1, anti-Sox10 and anti-Pdgfra followed by detection of EdU using the Alexa Fluor 555 Click-iT detection kit (Invitrogen).

***In situ* hybridization.** Our ISH protocols are available at http://www.ucl.ac.uk/~ucbzwdr/Richardson.htm and in ref. 47. Briefly, digoxigenin (DIG)- or fluorescein (FITC)-labeled RNA probes were transcribed *in vitro* from cloned cDNAs for mouse *Mbp* (DIG or FITC), *Pdgfra* (FITC) and *Enpp6* (DIG). For single-probe ISH, the DIG or FITC signal was visualized with alkaline phosphatase (AP)-conjugated anti-DIG or anti-FITC Fab2 fragments and a mixture of nitroblue tetrazolium (NBT) and 5-bromo-4-chloro-3-indolyl phosphate (toluidine salt) (BCIP) (all reagents from Roche Molecular Biochemicals). For double-fluorescence ISH, two probes, one FITC labeled and the other DIG labeled, were applied to sections simultaneously. The FITC signal was visualized by tyramide signal amplification (TSA) fluorescence system (NENTM Life Science Products, Boston) according to the manufacturer's instructions using horseradish peroxidase (HRP)-conjugated anti-FITC-POD antibody. After that, the DIG signal was visualized by a Fast Red fluorescence system (Roche) according to the manufacturer's instructions using AP-conjugated anti-DIG Fab2 antibody. For combined immunolabeling/ISH, immunolabeling was carried out after the ISH signal had been developed using Fast Red or TSA. For Mag and Mbp immunolabeling after ISH, the sections were heated at 95 °C for 20 min in 0.01 M citrate acid buffer (in diethyl-pyrocarbonate-treated water) before incubating with the *Enpp6* probe, then developing the signal with tyramide. After blocking with normal goat serum, the sections were incubated with rat anti-Mbp and mouse anti-Mag for 3 d at 4 °C before the secondary antibodies (Alexa Fluor 647 anti-rat IgG and Alexa Fluor 568 anti-mouse IgG). For double *Enpp6* and *Mbp* ISH followed by Mbp immunolabeling, the *Mbp* signal was first developed using TSA, then the *Enpp6* signal with Fast Red, then the anti-Mbp was added for 3 d at 4 °C before the Alexa Fluor 647 anti-rat IgG.

Statistics. No statistical methods were used to pre-determine sample sizes, but our sample sizes are similar to those reported in previous publications[8,21,30]. Mice were randomly assigned to experimental groups (for example, runners or nonrunners) with approximately equal numbers of female and male mice in each group. Prism 6.0 software (GraphPad) was used for statistical analysis. Running wheel data were analyzed by calculating average speed (m/min) for individual mice over different time windows, then mean ± s.e.m. for the whole experimental group over the same period. To assess differences between experimental cohorts at a given point in a time series (**Fig. 1** and **Supplementary Fig. 1**) we used two-way ANOVA with Bonferroni's *post hoc* tests. For comparing experimental cohorts at a single time point (**Figs. 2**, **6** and **7**), we used the two-tailed unpaired *t*-test. Cell counts are displayed as mean ± s.e.m. All cell counts in **Figures 2**, **6** and **7** were carried out by L.X., blinded as to whether the mice were runners or nonrunners. For key experiments (**Fig. 6j**,**k**; 2.5 h, 4 h and 12 h time points) cells were also counted independently by W.D.R., in a blinded fashion, with similar results (data not shown). Data from runners and nonrunners were compared by two-tailed unpaired *t*-test using GraphPad Prism 6.0. The variances of each pair of data sets being compared were similar to each other and consistent with their being normally distributed (assessed by Kolgomorov-Smirnov test: http://www.physics.csbsju.edu/stats/KS-test.n.plot_form.html). No animals or data points were excluded from the analysis.

A **Supplementary Methods Checklist** is available.

Data availability. The data that support the findings of this study are available from the corresponding author on request.

47. Jolly, S., Fudge, A., Pringle, N., Richardson, W.D. & Li, H. Combining double fluorescence in situ hybridization with immunolabelling for detection of the expression of three genes in mouse brain sections. *J. Vis. Exp.* **109** doi:10.3791/53976 (2016).